Spectrochimica Acta Part A: Molecular and Biomolecular Spectroscopy xxx (2014) xxx–xxx

Contents lists available at ScienceDirect

Spectrochimica Acta Part A: Molecular and Biomolecular Spectroscopy

journal homepage: www.elsevier.com/locate/saa

Synthesis, spectral behaviour and photophysics of donor–acceptor kind of chalcones: Excited state intramolecular charge transfer and fluorescence quenching studies

Mehboobali Pannipara [a], Abdullah M. Asiri [a,b], Khalid A. Alamry [a], Muhammad N. Arshad [a,b], Samy A. El-Daly [a,c,*]

[a] *Department of Chemistry, Faculty of Science, King Abdulaziz University, P.O. Box 80203, Jeddah 21589, Saudi Arabia*
[b] *Center of Excellence for Advanced Materials Research, King Abdulaziz University, P.O. Box 80203, Jeddah 21589, Saudi Arabia*
[c] *Department of Chemistry, Faculty of Science, Tanta University, 31527 Tanta, Egypt*

HIGHLIGHTS

- Chalcones with electron donor acceptor group has been studied.
- The absorption and emission spectrum were sensitive to solvent polarity.
- Fluorescence quantum yield highly depend on polarity of solvents.
- Both chalcones show fluorescence quenching by silver nanoparticles.

GRAPHICAL ABSTRACT

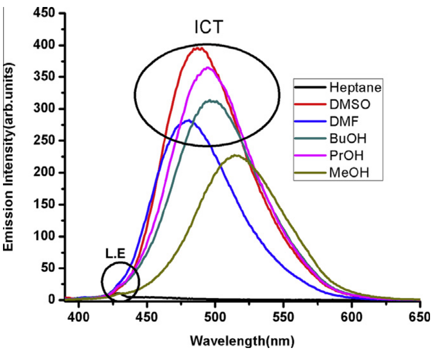

ARTICLE INFO

Article history:
Received 29 July 2014
Received in revised form 13 October 2014
Accepted 23 October 2014
Available online xxxx

Keywords:
Chalcones
Photophysics
Effect of solvent polarity
Silver nanoparticles

ABSTRACT

The spectral and photophysical properties of two chalcones containing electron donating and accepting groups with intramolecular charge transfer characteristics were synthesized and characterized by ^{1}H NMR, ^{13}C NMR and X-ray crystallography. Both compounds show very strong solvent polarity dependent changes in their photophysical characteristics, namely, remarkable red shift in the emission spectra with increasing solvent polarity, large change in Stokes shift, significant reduction in the fluorescence quantum yield; indicating that the fluorescence states of these compounds are of intramolecular charge transfer (ICT) character. The solvent effect on the photophysical parameters such as singlet absorption, molar absorptivity, oscillator strength, dipole moment, fluorescence spectra, and fluorescence quantum yield of both compounds have been investigated comprehensively. For both dyes, Lippert–Mataga and Reichardt's correlations were used to estimate the difference between the excited and ground state dipole moments ($\Delta\mu$). The interactions of dyes with colloidal silver nanoparticles (Ag NPs) were also studied in ethanol using steady state fluorescence quenching measurements. The fluorescence quenching data reveal that dynamic quenching and energy transfer play a major role in the fluorescence quenching of dyes by Ag NPs.

---

* Corresponding author at: King Abdulaziz University, P.O. Box 80302, Jeddah 21589, Saudi Arabia. Tel.: +966 554953522.
E-mail address: samyeldaly@yahoo.com (S.A. El-Daly).

http://dx.doi.org/10.1016/j.saa.2014.10.105
1386-1425/

Please cite this article in press as: M. Pannipara et al., Synthesis, spectral behaviour and photophysics of donor–acceptor kind of chalcones: Excited state intramolecular charge transfer and fluorescence quenching studies, Spectrochimica Acta Part A: Molecular and Biomolecular Spectroscopy (2014), http://dx.doi.org/10.1016/j.saa.2014.10.105

Introduction

Organic molecules featuring intramolecular charge transfer (ICT) has gained a substantial research interest owing to its potential application in making photoelectronic and nonlinear optical devices [1,2], chemical sensing [3], understanding photochemical and photobiological processes [4,5]. Pi-conjugated organic fluorophores containing donor acceptor groups that are separated by an ethenyl or keto-vinyl bridge, exhibiting the phenomenon of dual fluorescence are of special interest because the material properties can be tuned and tailored by structural modification for their potential applications in molecular electronics, dye sensitised solar cells [6,7] and other all optical devices [8,9]. The highly polar excited states and large charge separation exhibited by these molecules are sensitive to changes in its micro environment such as pH, viscosity, polarity, heat and light that can be exploited in various fields.

Chalcones symbolize a class of organic compounds in which two aromatic planar rings are connected through a three carbon α, β-unsaturated carbonyl system, with significant biological activities have been observed over the past two decades including anti-ulcer, anti-cancer, anti-mitotic, anti-inflammatory, anti-malarial, anti-fungal, and anti-oxidant activities [10–13]. Apart from these very important medicinal applications, chalcones have interesting optical and spectral properties depending on the substituent attached to the aromatic rings that find applications in metal sensing, optoelectronic and nonlinear optical devices [14,2]. The asymmetrically substituted electron-donating and electron-accepting substituents in these molecules are connected through a pi-conjugated system of alternate single and double bonds and exhibit different degrees of charge transfer in the ground and excited states. The photophysical properties of these conjugate intramolecular charge transfer compounds strongly depend on the nature of the substituent, solvent polarity and temperature.

Metallic nanoparticles possess unique spectroscopic, electronic and chemical properties due to their small size and high surface to volume ratios that are different from those of the individual atoms as well as their bulk counterparts. The optical properties of noble metal nano particles have received considerable attention because the surface plasmon absorption band of noble metal nanoparticles appears in the visible region of the spectrum to provide important contribution towards sensing and bio-medical applications. Interaction of metallic nanoparticles (NPs) with fluorophores has become an active area of research for the last two decades with applications ranging from material science to biomedical science [15–17]. The fluorescence of a dye molecule is quenched or enhanced in the close proximity of the metallic nanoparticles and these phenomena can be used to probe the micro environment of the fluorophore. The emission behaviour of a dye molecule can be altered by using metallic nanoparticles and quenching or enhancement of photoluminescence of a dye by silver nanoparticles (AgNPs) depend upon the distance between the dye molecule and NPs [18–20]. The quenching processes are of three types: static, dynamic and by electron/energy transfer. In static quenching, the decrease in emission intensity is caused by the adsorption of dye molecule on the surface of the metallic NPs, forming a non fluorescent complex between the fluorophore and quencher where as in dynamic quenching, the reduction of emission intensity is due to the direct interaction or collision of excited fluorophore with a quencher during their excited state life time. The third type of quenching process takes place by non-radiative energy/electron transfer between the dye molecule and NPs [21,22]. The quenching of fluorescence dominates over enhancement at shorter distances and it is attributed to the efficient non-radiative energy transfer between the dye molecule and the metallic NP [23].

The present work aims at setting up a scheme which can efficiently predict the excited state intramolecular charge transfer process applying steady state spectroscopy, quantum yield calculation with variation of polarity of the solvents. For this purpose, we have synthesized and characterized two chalcone derivatives, namely, 3-(1-Benzyl-1*H*-3-indol-3-yl)-1-naphthalen-2-yl-propenone and 3-(1-Benzyl-1*H*-3-indol-3-yl)-1-thiophene-3-yl-propenone; and studied the effect of solvents in detail. Lippert–Mataga and Reichardt's correlations were applied to calculate the difference between the excited and ground state dipole moments ($\Delta\mu$). To explore the effect of metallic nanoparticles with the synthesized fluorophores, we also investigate fluorescence quenching by colloidal silver nanoparticles in ethanol using steady state emission measurements.

Experimental

Materials and methods

All solvents and chemicals used in this work were of spectroscopic grade obtained from Sigma–Aldrich and used without further purification. Synthetic procedure and characterization of silver nanoparticles are given in the supporting information and TEM image of Ag NPs with absorption spectrum shown as an inset in Fig. S1. Indole-3-carbaldehyde, 3-acetylthiophene and 2-acetonaphthone were purchased from Sigma–Aldrich.

Spectral measurements

All solvents and chemicals used in this work were of spectroscopic grade obtained from Sigma Aldrich and used without further purification. Melting points were determined on a Gallenkamp melting point apparatus and the infrared (IR) spectra were recorded on Shimadzu FT-IR 8400S infrared spectrophotometer using the KBr pellet technique. The NMR (^{1}H and ^{13}C) spectra were recorded on a Bruker DPX-600 at 600 MHz and 150 MHz, respectively, using tetramethylsilane as the internal standard. The chemical shift values are recorded on δ scale and coupling constants (J) in Hertz; Splitting patterns were designated as follows: *s*: singlet; *d*: doublet; *m*: multiplet. UV–Vis electronic absorption spectra was recorded on a Shimadzu UV-160A spectrophotometer, and the steady-state fluorescence spectra were measured using Shimadzu RF 5300 spectrofluorphotometer using a rectangular quartz cell of dimensions 0.2 cm × 1 cm. The emission was monitored at right angle. The fluorescence quantum yield (ϕ_f) was measured using an optically diluted solution of quinine sulfate as reference according to Eq. (1):

$$\phi_u = \phi_s \times \frac{I_u}{I_s} \times \frac{A_s}{A_u} \times \frac{n_u^2}{n_s^2} \tag{1}$$

where ϕ_u, ϕ_s are the fluorescence quantum yields of the unknown and standard, respectively, I is the integrated emission intensity; A is the absorbance at excitation wavelength, and n is the refractive index of the solvent. The subscript u and s refers to unknown and standard, respectively.

Procedure for the synthesis of 1-Benzyl-1H-3-indolecarbaldehyde **(2)**

To a solution of indole-3-carbaldehyde (1.5 g, 0.010 mol) in ethanol (50 mL), KOH pellets were added (0.69 g, 0.012 mol) and the mixture were stirred at room temperature until total solubilisation. The ethanol was completely removed in vacuum and acetone (50 mL) was added followed by benzyl bromide (0.010 mol, 1.2 mL). A precipitate was formed instantly on addition of benzyl bromide

Please cite this article in press as: M. Pannipara et al., Synthesis, spectral behaviour and photophysics of donor–acceptor kind of chalcones: Excited state intramolecular charge transfer and fluorescence quenching studies, Spectrochimica Acta Part A: Molecular and Biomolecular Spectroscopy (2014), http://dx.doi.org/10.1016/j.saa.2014.10.105

and the solid was filtered and the solution was concentrated in vacuum and crystallized from ethanol to give **2** (2.1 g, 92%) as brown solid.

Brown solid, m.p: 100–1020C; ^{1}H NMR (600 MHz, DMSO-d6) δ 5.4 (*s*, 2H), 7.25–8.12 (*m*, 9H), 8.55 (*s*,1H), 10.2 (*s*,1H); IR (KBr, cm^{-1}): υmax = 1652, 2954.

*Procedure for the synthesis of 3-(1-Benzyl-1H-3-indol-3-yl)-1-naphthalen-2-yl-propenone (BNP) (**3a**)*

A solution of 1-Benzyl-1*H*-3-indolecarbaldehyde (1 g, 0.0042 mol) and 2-acetonaphthone (0.71 g, 0.0042 mol) in an ethanolic solution of NaOH (2 g in 20 mL ethanol) was stirred for 3–5 h at room temperature and allowed to stand overnight. The solid product was collected by filtration, dried and recrystallized from ethanol to give **3a** (1.36 g, 82%) as yellow solid.

Yellow solid, m.p: 182–1840C; ^{1}H NMR (600 MHz, CDCl3) δ 5.37 (*s*, 2H), 7.25–8.12 (*m*, 9H), 8.55 (*s*, 1H), 7.73 (*d*, 1H, *J* = 15.4 Hz), 7.37 (*d*, 1H, *J* = 15.1 Hz), 7.32 (*s*, 1H), 7.55–7.61 (*m*, 3H), 7.18 (*d*, 2H, *J* = 7.2 Hz), 8.16 (*d*, 1H, *J* = 8 Hz); ^{13}C NMR (150 M Hz, CDCl3) δ 190.05, 138.5, 137.8, 136.4, 136.0, 135.2, 133.7, 132.7, 129.5, 129.3, 129.0, 128.8, 128.3, 128.1, 128.0, 127.8, 127.0, 126.7, 126.6, 124.7, 123.3, 121.7, 120.9, 118.1, 117.6, 113.6, 110.7, 50.6; IR (KBr, cm^{-1}): υmax = 1648, 1540, 1180, 1020.

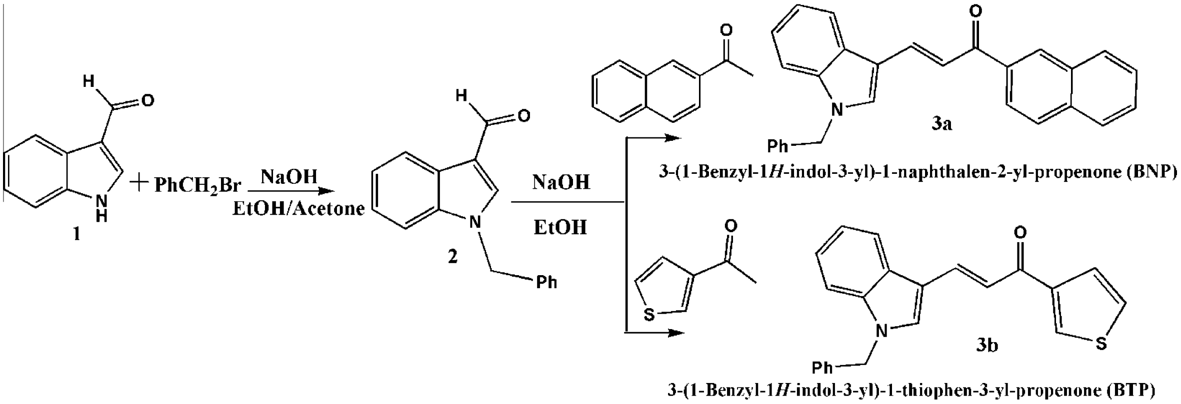

Scheme 1. Synthetic route to synthesized chalcones.

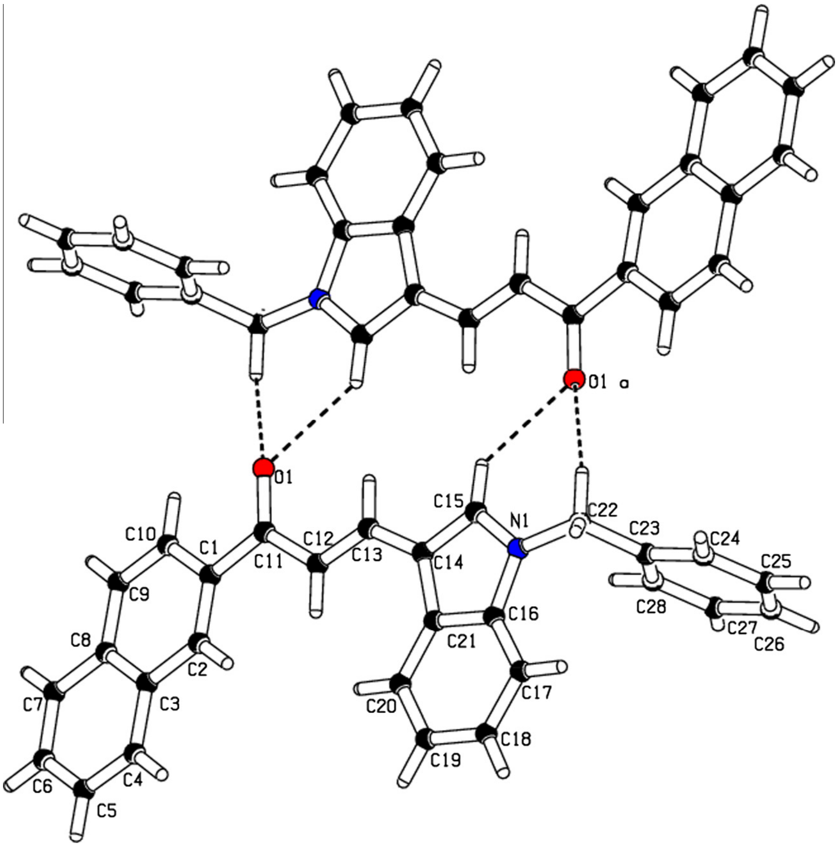

Fig. 1. Labelled diagram of **3a** showing inter molecular hydrogen bonding using dashed lines.

Please cite this article in press as: M. Pannipara et al., Synthesis, spectral behaviour and photophysics of donor–acceptor kind of chalcones: Excited state intramolecular charge transfer and fluorescence quenching studies, Spectrochimica Acta Part A: Molecular and Biomolecular Spectroscopy (2014), http://dx.doi.org/10.1016/j.saa.2014.10.105

*Procedure for the synthesis of 3-(1-Benzyl-1H-3-indol-3-yl)-1-thiophene-3-yl-propenone (BTP) (**3b**)*

A solution of 1-Benzyl-1*H*-3-indolecarbaldehyde (1 g, 0.0042 mol) and 3-acetylthiophene (0.53 g, 0.0042 mol) in an ethanolic solution of NaOH (2 g in 20 mL ethanol) was stirred for 3–5 h at room temperature and allowed to stand overnight. The solid product was collected by filtration, dried and crystallized from ethanol to give **3b** (1.2 g, 86%) as brown solid.

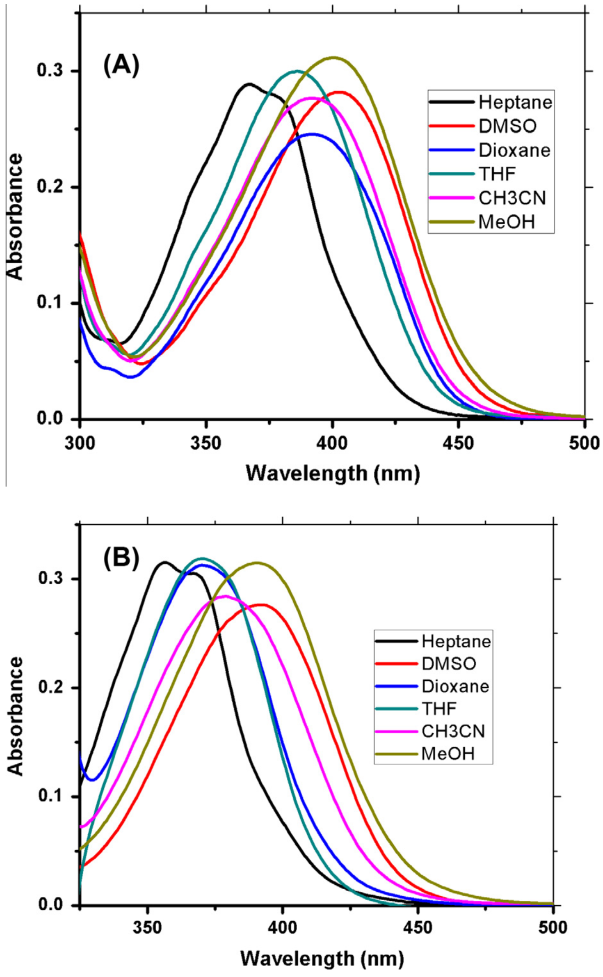

Fig. 2. Electronic absorption spectra of (1×10^{-5} M) **3a** (Panel A) and **3b** (Panel B) in different solvents.

Brown solid, m.p: 160–1620C; ^{1}H NMR (600 MHz, CDCl3) δ 5.4 (*s*, 2H), 7.25–8.12 (*m*, 9H), 8.55 (*s*, 1H), 7.53 (*d*, 1H, *J* = 14.2 Hz), 7.26 (*d*, 1H, *J* = 15.1 Hz), 7.22 (*s*, 1H), 7.08 (*d*, 1H, *J* = 7.2 Hz), 7.12 (*d*, 1H, *J* = 7.2 Hz); ^{13}C NMR (150 M Hz, CDCl3) δ 190.1, 150.1, 142.2, 140.1,137.8, 137.4, 130.1,130.4, 130.4, 127.8, 124.6, 127.6, 125.2, 129.4, 129.4, 128.5, 122.2, 112.4, 120.8, 110.4, 102.8, 50.2; IR (KBr, cm^{-1}): υmax = 1648, 1540, 1180, 1020.

*X-ray crystal structure of **3a***

Single crystal of **3a** suitable for X-ray analysis was obtained at room temperature by slow evaporation of ethanol and water mixture of the compound. One crystal of **3a** (yellow 0.30 × 0.20 × 0.10 mm) was mounted on Agilent Supernova (Dual source) Agilent Technologies Diffract meter, equipped with a graphite-monochromatic Cu Kα radiation (λ = 1.54184), to collect diffraction data using CrysAlisPro software at 296 K. The structure solution was achieved through SHELXS-97 [24] and refined by full-matrix least-squares methods on F^2 using SHELXL-97, in-built with X-Seed [25]. All the C–H hydrogen atoms were positioned geometrically and treated as riding atoms with $C_{aromatic}$–H = 0.93, C_{methyl}–H0.96 Å and refined using a riding model with Uiso (H) = 1.5 Ueq (C) for methyl and Uiso (H) = 1.2 Ueq (C) for all other carbon atoms. CCDC 980984 contains the supplementary crystallographic data for this paper. These data can be obtained free of charge at www.ccdc.cam.ac.uk/conts/retrieving.html or from the Cambridge Crystallographic Data Centre, 12 Union Road, Cambridge CB2 1EZ, UK.

Results and discussion

Chemistry

We have synthesized and characterized two chalcone derivatives having intramolecular charge transfer characteristics, namely, 3-(1-Benzyl-1*H*-3-indol-3-yl)-1-naphthalen-2-yl-propenone (**3a**) and 3-(1-Benzyl-1*H*-3-indol-3-yl)-1-thiophene-3-yl-propenone (**3b**). The changes in dipole moments were calculated using Lippert–Mattaga and Reichardt's correlations. The solvent effect on the absorption and emission spectra were investigated in detail with solvents having different polarity. Scheme 1 outlines the synthetic route to the synthesis of two chalcone derivatives. Compound **2** was synthesized by N-alkylation indole-3-aldehyde with 1 equivalent benzyl bromide in presence of NaOH as base and ethanol as solvent. Compound **3a** and **3b** were obtained by Claisen–Schmidt aldol condensation of compound **2** with 3-acetylthiophene and 2-acetonaphthone in presence of one equiv. of NaOH in ethanol. The structures of compounds were confirmed by IR, ^{1}H NMR and ^{13}C NMR.

Table 1
Spectral and photophysical parameters of **3a** in different solvents.

Solvents	λ_{abs} (nm)	λ_{em} (nm)	$\Delta\bar{\nu}$ (cm^{-1})	ε M^{-1} cm^{-1}	ϕ_f	f	μ_{12} Debye	$E_T(30)$ K cal mol^{-1}	Δf (D, n)	E_T^N
Toluene	382	432	3029	27160	0.03	0.56	6.75	33.9	0.0132	0.099
Heptane	367	430	3992	28860	0.0092	0.58	6.70	31.1	0.0004	0.006
DMSO	404	490	4344	28190	0.35	0.56	6.93	45.1	0.263	0.441
Dioxane	394	454	3354	24540	0.029	0.52	6.61	36	0.021	0.164
THF	387	461	4147	29980	0.047	0.64	7.27	37.4	0.210	0.210
Ethyl Acetate	382	463	4579	28750	0.04	0.61	7.03	38.1	0.199	0.230
Acetonitrile	391	482	4828	27660	0.41	0.61	7.10	45.6	0.304	0.472
Chloroform	394	471	4149	26380	0.137	0.57	6.87	39.1	0.148	0.259
DMF	402	481	4085	26390	0.267	0.53	6.72	43.8	0.274	0.404
Butanol	402	498	4795	29520	0.263	0.64	7.40	50.2	0.263	0.506
Propanol	404	495	4550	29690	0.306	0.63	7.35	49.2	0.274	0.570
Ethanol	403	508	5128	30090	0.314	0.63	7.35	51.9	0.288	0.654
Methanol	401	515	5520	31160	0.18	0.68	7.62	55.4	0.308	0.762

Please cite this article in press as: M. Pannipara et al., Synthesis, spectral behaviour and photophysics of donor–acceptor kind of chalcones: Excited state intramolecular charge transfer and fluorescence quenching studies, Spectrochimica Acta Part A: Molecular and Biomolecular Spectroscopy (2014), http://dx.doi.org/10.1016/j.saa.2014.10.105

*Single crystal structure of **3a***

Single crystal analysis of compound **3a** reveals that the molecule forms a monoclinic crystal pattern with P21/n space group. The molecule contains naphthalene, indole and a phenyl ring system in its skeleton. The structural studies along with the other physical studies were carried out to know the three dimensional behaviour of molecules and Vander-Walls interactions in a unit cell. The naphthalene and indole moieties are making a curve with the dihedral angle of 8.29(1)°. The phenyl ring is almost perpendicular to naphthalene and indole systems and the dihedral angles are 81.12(1)° and 79.06(7)°, respectively. The molecules are further stabilized by weak C–H···O interactions and form inversion dimers via the formation of two five membered ring motifs R_2^1 (5) [26] as shown in Fig. 1. The crystallographic data and refinement parameters are available in Table S1 (supporting information) and the bond lengths and bond angles are provided in Tables S2 and S3 (supporting information). In this intermolecular interaction, the oxygen atom is situated at $(1 - x, 1 - y, -z)$ with respect to the donor carbon atoms (C15 & C22) at (x, y, z) via H15 & H22B respectively (Table S4).

*Solvent effect on absorption and emission spectra of **3a** and **3b***

Absorption spectra of compound **3a** and **3b** (1×10^{-5} M) were recorded in solvents of different polarity show slight variation in the absorption maxima on going from polar aprotic solvents to polar protic solvents. Representative absorption spectra of both compounds recorded in some selective solvents are shown in Fig. 2 and the corresponding spectral data are summarized Tables 1 and 2. An overall red shift of 38 nm is observed in the absorption maxima of both compounds on going from heptane to methanol suggesting some polar character in the ground state. In all alcoholic solvents, both compounds show a red shifted broad absorption band indicating that the allowed transition is π–π^* with charge transfer character. On excitation at 365 nm, the emission spectrum of both **3a** and **3b** show smooth correlation with increasing polarities of the solvents (Fig. 3; Tables 1 and 2). A remarkable red shift of 85 nm is observed for compound **3a** on going from heptane to methanol, where as the shift is 70 nm for compound **3b**; suggesting the involvement of photo induced intramolecular charge transfer (ICT) in the singlet excited state from the electron donating group to electron accepting keto group with larger dipole moment in the excited state than in ground state. In case of both compounds only one emission peak is observed in non polar solvents like heptane and toluene at $\sim$430 nm, but in polar solvents a large red shifted emission band is observed within the wavelength range $\sim$455–515 nm for compound **3a** and $\sim$446–499 nm for **3b** in addition to the short wave length band. This kind of dual emission is characteristic of compounds containing electron donor and acceptor group constituted of a conjugated π-electron system. The red shifted band in polar solvents arises from the charge transfer state and short wavelength emission band ($\sim$430 nm) originate from a locally excited state and appears almost at the same position as the maximum in non polar solvents (Fig. 3). Moreover, in solvents having almost equal polarity like acetonitrile and methanol (expressed in Δf), compound **3a** shows a red shift of 33 nm in methanol ($\sim$515 nm) from that of the emission band in acetonitrile solvent ($\sim$482 nm) (Fig. 3) and compound **3b** show a

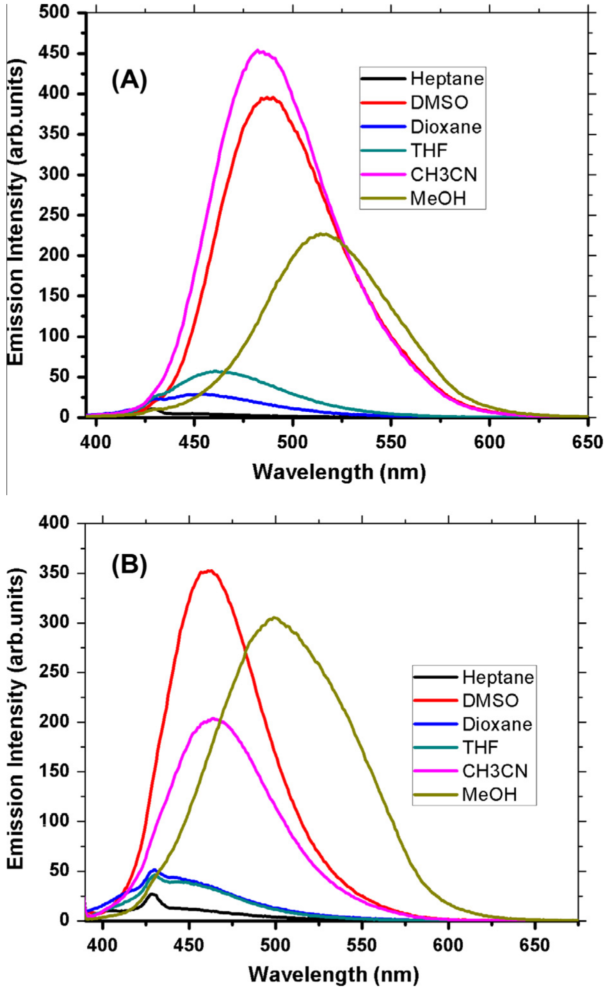

Fig. 3. Emission spectra of (1×10^{-5} M) **3a** (Panel A) and **3b** (Panel B) in different solvents.

Table 2
Spectral and photophysical parameters of **3b** in different solvents.

Solvents	λ_{abs} (nm)	λ_{em} (nm)	$\Delta\bar{\nu}$ (cm^{-1})	ε M^{-1} cm^{-1}	ϕ_f	f	μ_{12} Debye	$E_T(30)$ K cal mol^{-1}	$\Delta f\,(D, n)$	E_T^N
Toluene	379	430	3129	26150	0.051	0.54	6.60	33.9	0.0132	0.099
Heptane	356	429	4780	31520	0.021	0.58	6.60	31.1	0.0004	0.006
DMSO	391	461	3883	27650	0.32	0.55	6.73	45.1	0.263	0.441
Dioxane	370	430	3771	31270	0.041	0.59	6.79	36	0.021	0.164
THF	370	431	3825	31900	0.036	0.59	6.80	37.4	0.210	0.210
Ethyl Acetate	370	446	4606	29370	0.049	0.57	6.69	38.1	0.199	0.230
Acetonitrile	379	464	4834	28410	0.18	0.59	6.88	45.6	0.304	0.472
Chloroform	386	461	4215	25820	0.11	0.54	6.66	39.1	0.148	0.259
DMF	384	457	4160	28710	0.17	0.58	6.88	43.8	0.274	0.404
Butanol	393	479	4568	29330	0.22	0.60	7.05	50.2	0.263	0.506
Propanol	391	475	4523	31030	0.24	0.63	7.21	49.2	0.274	0.570
Ethanol	395	495	5114	30330	0.27	0.61	7.13	51.9	0.288	0.654
Methanol	390	499	5601	31490	0.24	0.65	7.34	55.4	0.308	0.762

Please cite this article in press as: M. Pannipara et al., Synthesis, spectral behaviour and photophysics of donor–acceptor kind of chalcones: Excited state intramolecular charge transfer and fluorescence quenching studies, Spectrochimica Acta Part A: Molecular and Biomolecular Spectroscopy (2014), http://dx.doi.org/10.1016/j.saa.2014.10.105

red shift of 35 nm. This clearly indicates that apart from polarity effect, hydrogen bonding effect is also responsible for the red shift with increasing hydrogen bonding ability of solvents from 1-propanol to methanol.

*Fluorescence quantum yield of **3a** and **3b** in different solvents*

Fluorescence quantum yield values give an insight on the photophysical properties of an unknown fluorescent molecule. The fluorescence quantum yield (ϕ_f) of both compounds are strongly influenced by the polarity and hydrogen bonding ability of the solvents as shown in Tables 1 and 2. The fluorescence quantum yield can be correlated with $E_T(30)$ of the solvent, where $E_T(30)$ is the solvent polarity parameter introduced by Reichardt [27], that considers interactions such as solvent polarizability and hydrogen bonding besides those of a specific nature. As depicted in Fig. 4, ϕ_f increases with increase in the polarity of the solvent (expressed as $E_T(30)$); reaching maximum in polar aprotic solvents like acetonitrile for **3a** and in DMSO for that of **3b** with a drop on further increase in the solvent polarity such as in alcoholic solvents. The increase in ϕ_f (negative solvatokinetic effect) with charge transfer character was explained by several mechanisms such as proximity effect and conformational changes [28]. Hydrogen bonding between solvent molecules and the carbonyl group of fluorophore is accounted for the reduction of ϕ_f in highly protic alcoholic solvents due to enhanced radiationless processes. The reduction in ϕ_f going from DMSO to polar protic solvents like MeOH (positive solvatokinetic effect) can be attributed to strong ICT interaction, the ϕ_f value decrease strongly in highly proton donor solvents. This effect is due to inter molecular hydrogen bonding interaction between solvent and excited dyes. Hydrogen bonding will induce fluorescence quenching due to the enhancement of intersystem crossing, strong internal conversion and vibrational deactivation [29–32].

Estimation of dipole moments using solvatochromic methods

The degree of charge distribution in a molecule used to clarify a variety of physical and chemical properties. Lippert–Mataga' Eqs. (2) and (3) [33,34], which is based on the correlation of energy difference between the ground and excited states (Stokes' shift) with the solvent orientation polarizability (Δf), can be used to investigate the change in dipole moment between the excited singlet state and ground state.

$$\Delta\bar{\nu}_{st} = \frac{2(\mu_e - \mu_g)^2}{hca^3}\Delta f + Const. \qquad (2)$$

$$\Delta f = \frac{\varepsilon - 1}{2\varepsilon + 1} - \frac{n^2 - 1}{2n^2 + 1} \qquad (3)$$

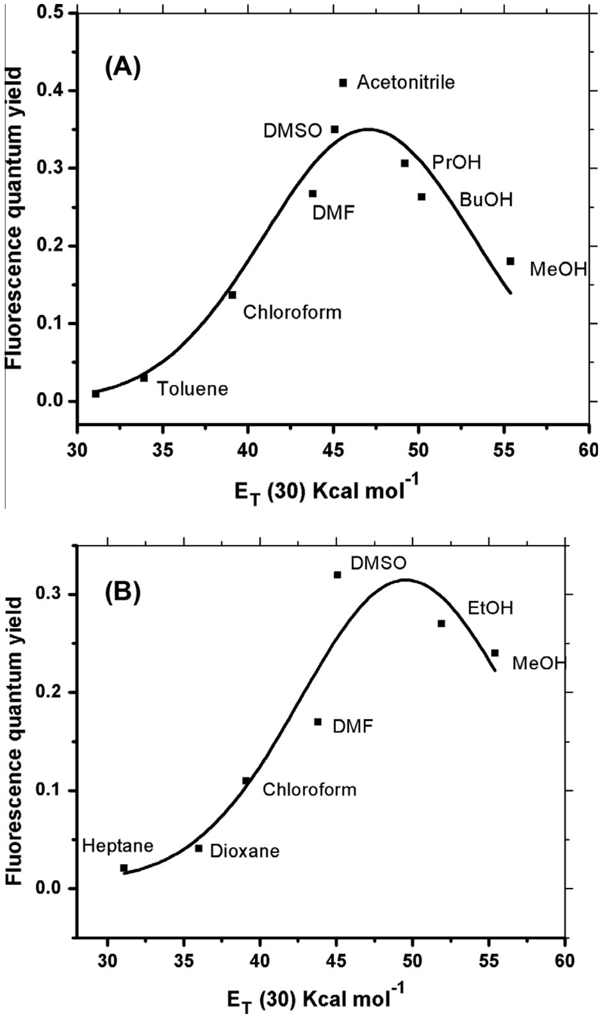

Fig. 4. Plot of $E_T(30)$ versus fluorescence quantum yield for **3a** (Panel A) and **3b** (Panel B).

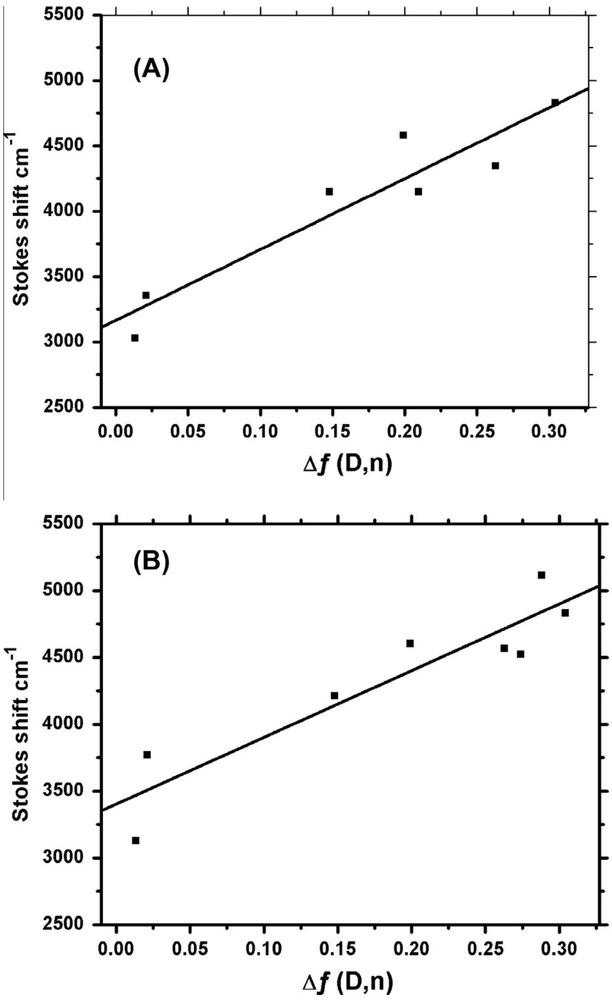

Fig. 5. Correlations of the Stokes' shift with the solvent polarity function (Δf) for **3a** (Panel A) and **3b** (Panel B).

Please cite this article in press as: M. Pannipara et al., Synthesis, spectral behaviour and photophysics of donor–acceptor kind of chalcones: Excited state intramolecular charge transfer and fluorescence quenching studies, Spectrochimica Acta Part A: Molecular and Biomolecular Spectroscopy (2014), http://dx.doi.org/10.1016/j.saa.2014.10.105

where $\Delta\bar{\nu}_{st}$ is the difference between the absorption and emission maxima expressed in wave numbers (cm^{-1}), respectively, h is Planck's constant, c is the speed of light in vacuum, a is the Onsager cavity radius, ε and n are the dielectric constant and refractive index of the solvent, respectively, μ_e and μ_g are the dipole moments in the excited and ground state, respectively, and Δf is the orientation polarizability of the solvent which measures both electron mobility and dipole moment of the solvent molecule. The Onsager cavity radii (a) from molecular volume of molecules is calculated by using Suppan's Eq. (4) [35]:

$$a = \left(\frac{3M}{4\pi\delta N}\right)^{1/3} \tag{4}$$

where δ is the density (obtained from crystallographic data) of dye, M is the molecular weight of dye and N is Avogadro's number. Fig. 5 shows the plots of Stokes shift versus the orientation polarization (Δf), and the change in dipole moment calculated for **3a** from the slop of this plot and cavity radius (a) is found to be 8.07 D and that of **3b** is 7.75 D. The data in polar protic solvents were excluded to avoid specific solute–solvent interactions (hydrogen bonding). The linear correlation of Lippert–Mataga plot supports the occurrence of photo induced intramolecular charge transfer in both compounds.

In addition, the change in dipole moment ($\Delta\mu$) between the excited singlet and ground state was also investigated using solvatochromic shift method [27,36], making use of the dimensionless microscopic solvent polarity parameters E_T^N given by the Eq. (5):

$$E_T^N = \frac{E_T(solvent) - 30.7}{32.4} \tag{5}$$

where λ_{max} corresponds to the peak wavelength in the red region of the intramolecular charge transfer absorption of the betaine dye. In this method, change in dipole moment is calculated by correlating the Stokes shift of the fluorophore to E_T^N (Fig. 6) according to Eq. (6).

$$\Delta\bar{\nu} = 11307.6\left(\frac{\Delta\mu}{\Delta\mu_D}\right)^2\left(\frac{a_D}{a}\right)^3 E_T^N + Const. \tag{6}$$

$\Delta\mu$ is the difference between the excited and ground state dipole moments of the probe molecule and $\Delta\mu_D$ is the change in the dipole moment of the betaine dye; a (taken as 4.35 Å) and a_D are the Onsager cavity radii a of the probe molecule and betaine molecule respectively. Since the values of a_D and μ_D are known (6.2 Å and 9 Debye, respectively) the change in dipole moment is calculated using Eq. (7),

$$\Delta\mu = \left[\frac{81m}{(6.2/a)^3 \times 11307.6}\right]^{1/2} \tag{7}$$

where m is the slope of linear plot of E_T^N vs. Stokes shift (Fig. 6) and the value for $\Delta\mu$ is found to be 3.67 D for **3a** and that of **3b** is 3.26 D. The value of $\Delta\mu$ obtained by Lippert–Mataga's equation is higher

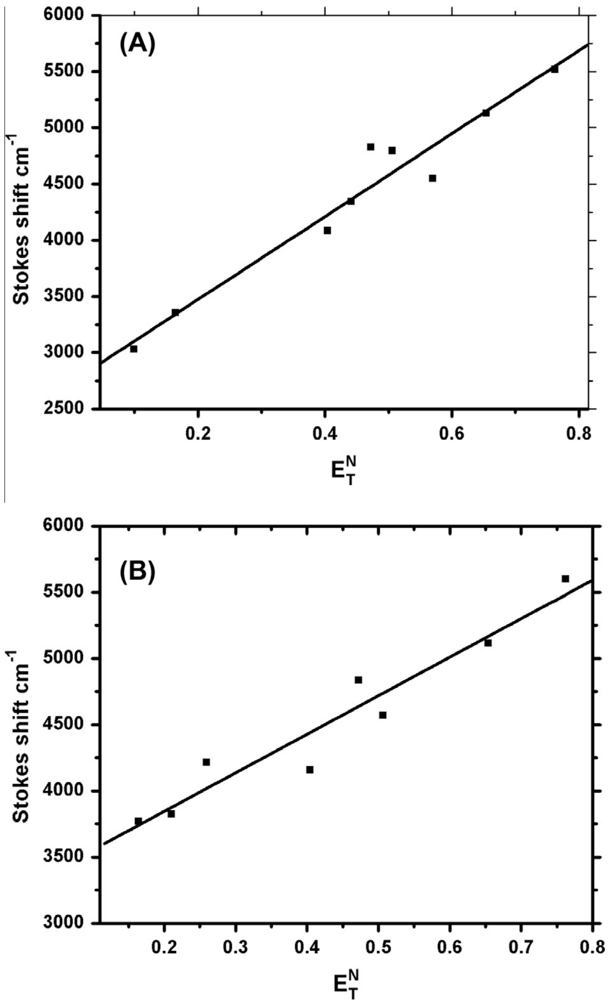

Fig. 6. Correlation of the Stokes' shift with E_T^N for **3a** (Panel A) and **3b** (Panel B).

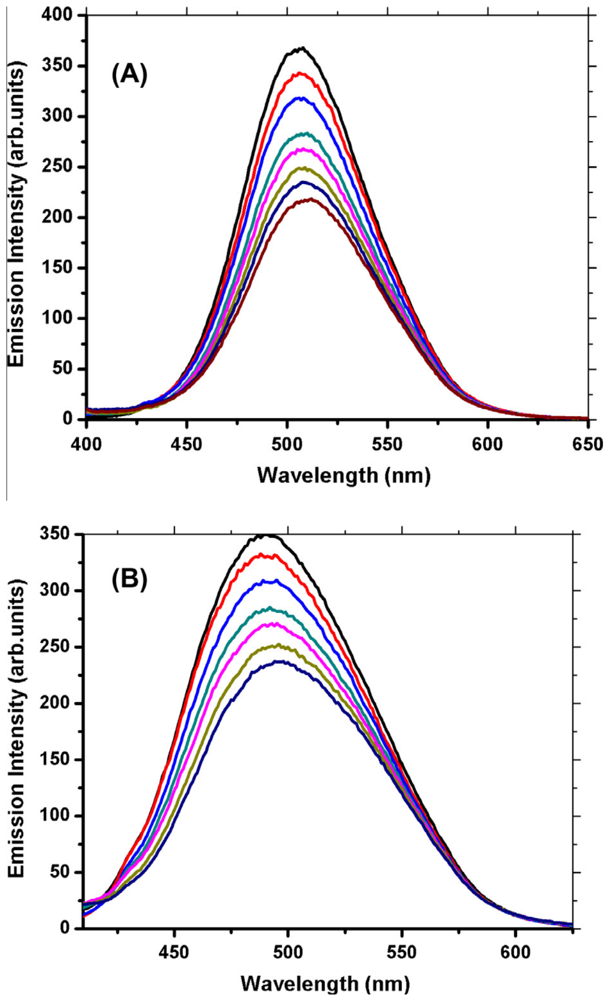

Fig. 7. (A) Emission spectra of 1×10^{-5} mol L^{-1} of **3a** in EtOH in presence of different concentrations of Ag NPs. The concentrations of Ag NPs at decreasing emission intensity are 0.0, 39, 78, 117, 156, 195, 234, and 312 pM (λ_{ex} = 380 nm). (B) Emission spectra of 1×10^{-5} mol L^{-1} of **3b** in EtOH in presence of different concentrations of Ag NPs. The concentrations of Ag NPs at decreasing emission intensity are 0.0, 39, 117, 156, 195, 273, and 312 pM (λ_{ex} = 380 nm).

Please cite this article in press as: M. Pannipara et al., Synthesis, spectral behaviour and photophysics of donor–acceptor kind of chalcones: Excited state intramolecular charge transfer and fluorescence quenching studies, Spectrochimica Acta Part A: Molecular and Biomolecular Spectroscopy (2014), http://dx.doi.org/10.1016/j.saa.2014.10.105

than that obtained by dimensionless microscopic solvent polarity parameters E_T^N , because in Lippert's plot only the dipole–dipole interactions are taken into account and does not consider the polarizability of solute molecules.

The ground to excited state transition dipole moment (μ_{12}) of **3a** and **3b** in different solvents was calculated using Eq. (8) [37]:

$$\mu_{12}^2 = \frac{f}{4.72 \times 10^{-7} E_{\max}} \tag{8}$$

where $E_{\max}$ is the energy maximum absorption in cm^{-1} and f is the oscillator strength which shows the effective number of electrons whose transition from ground to excited state gives the absorption area of the electronic spectrum. The experimental oscillator strength values were calculated using Eq. (9) [38]:

$$f = 4.32 \times 10^{-9} \int \varepsilon(\bar{v})\, d\bar{v} \tag{9}$$

where ε is the numerical value for molar decadic extinction coefficient measured in dm^3 mol^{-1} cm^{-1} and $\bar{v}$ is the numerical value of the wave number measured in cm^{-1}. The values of f and μ_{12} are listed in Table 1 and indicate that the $S_o \rightarrow S_1$ transition is strongly allowed.

*Fluorescence quenching study of **3a** and **3b** by silver nanoparticles*

The nature of molecular interaction and microenvironment of fluorophores in solution can be studied by fluorescence quenching experiments. Interaction of silver nanoparticles with **3a** and **3b** were investigated by fluorescence quenching measurements with variable concentrations of Ag NPs in ethanol. The emission spectra of 1×10^{-5} mol L^{-1} solution of **3a** and **3b** in ethanol with different concentrations of Ag NPs are shown in Fig. 7. On increasing the concentration of Ag NPs, the emission spectrum of **3a** and **3b** remains unaltered in wavelength but a substantial decrease in fluorescence intensity was observed; which rules out the possibility of ground state complex formation between dyes and Ag NPs.

The fluorescence quenching behaviour can be analyzed by the well-known Stern–Volmer equation. The Stern–Volmer quenching constant (K_{sv}) for **3a** and **3b** using Ag NPs as quencher were obtained from the Stern–Volmer Eq. (10) [39]:

$$\frac{I_o}{I} = 1 + K_{sv}[\mathrm{Ag^o}] \tag{10}$$

where I_o and I are the fluorescence intensities in the absence and presence of the quencher concentration [Ag^o]. The Stern–Volmer plot for **3a** and **3b** (Fig. 8) were found to be linear with correlation coefficient (R^2) equal to 0.99. From the slopes of the linear plots, K_{sv} values were calculated as 2.34×10^9 M^{-1} for **3a** and 1.52×10^9 M^{-1} for **3b**. The significant overlap between the emission spectrum of both dyes with the absorption of spectrum of Ag NPs (Fig. 9) reveal the possibility of non-radiative energy transfer from dyes to Ag NPs according to Forster's theory [40]. Thus, the Stern–Volmer plot and the spectral overlap between the both compounds and Ag NPs indicate the dynamic nature of the quenching process.

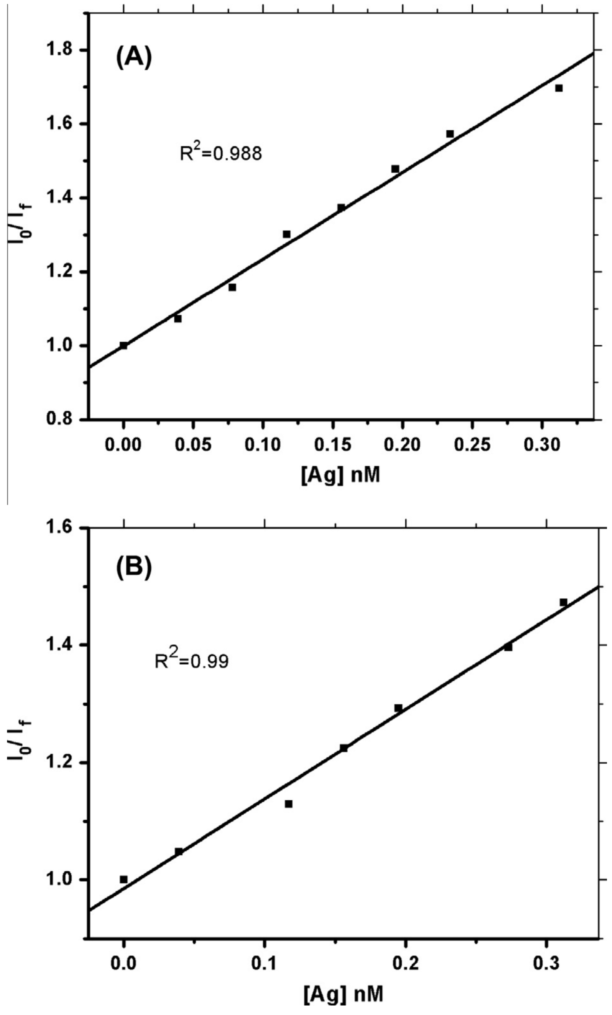

Fig. 8. Stern–Volmer plot for fluorescence quenching of **3a** (Panel A) and **3b** (Panel B) by Ag NPs in ethanol.

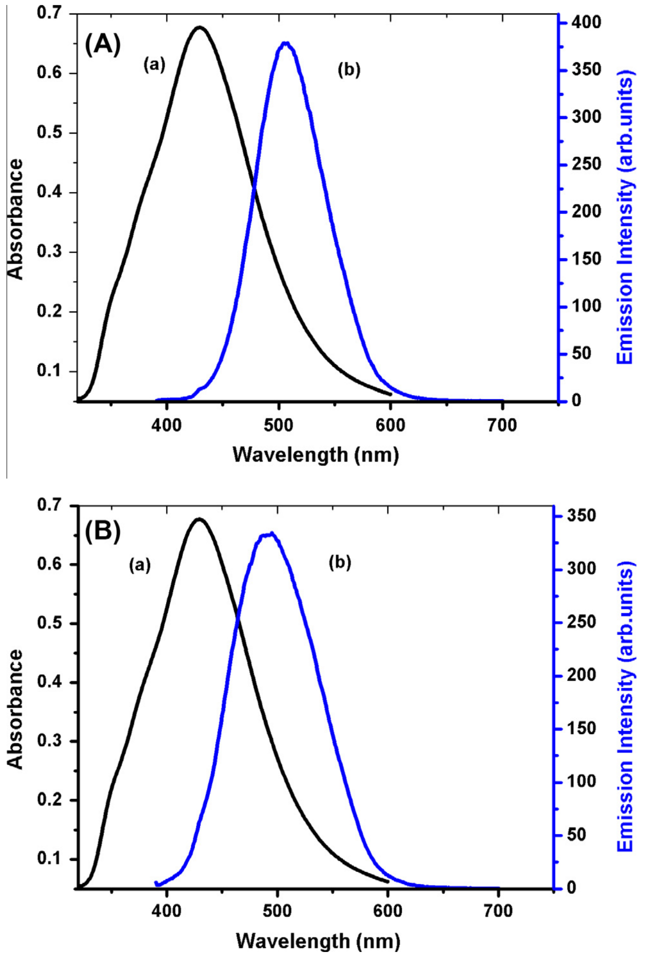

Fig. 9. Spectral overlap of (a) absorption spectrum of silver nanoparticles with and (b) emission spectrum of **3a** (Panel A) and **3b** (Panel B).

Please cite this article in press as: M. Pannipara et al., Synthesis, spectral behaviour and photophysics of donor–acceptor kind of chalcones: Excited state intramolecular charge transfer and fluorescence quenching studies, Spectrochimica Acta Part A: Molecular and Biomolecular Spectroscopy (2014), http://dx.doi.org/10.1016/j.saa.2014.10.105

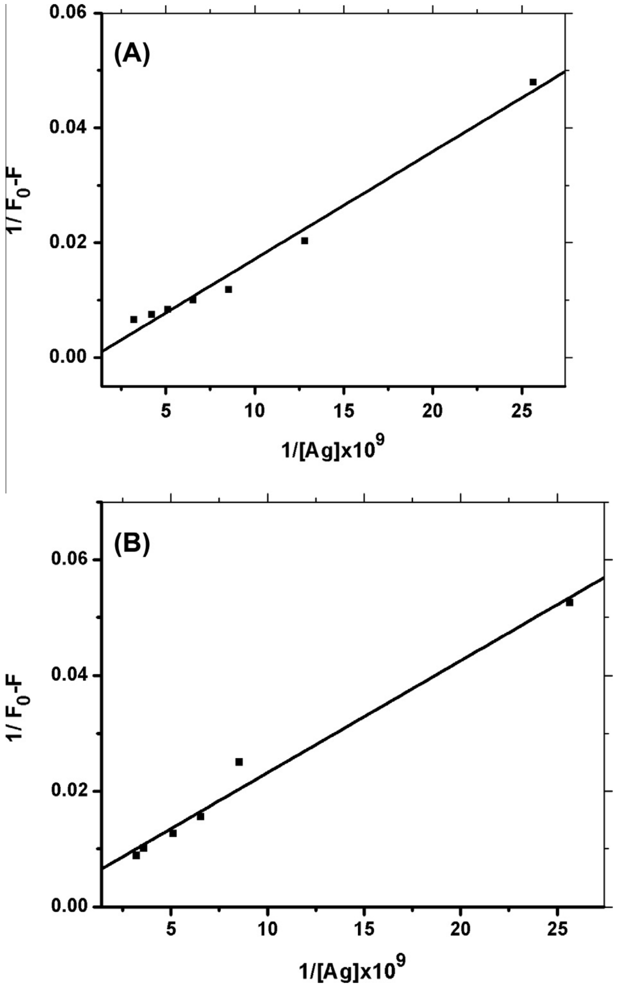

Fig. 10. Benesi–Hildebrand plot for the adsorption of **3a** on Ag NPs in ethanol (Panel A) and **3b** (Panel 3B).

The interaction between adsorbed and unadsorbed dye molecules was further investigated by determining the apparent association constant (K_{app}) using Benesi–Hildebrand method [41], Eqs. (11)–(13).

$$\mathrm{Dye} + \mathrm{Ag} \rightarrow [\mathrm{Dye} \cdots \mathrm{Ag}] \tag{11}$$

$$K_{app} = [\mathrm{Dye} \cdots \mathrm{Ag}]/[\mathrm{Dye}][\mathrm{Ag}] \tag{12}$$

$$\frac{1}{F^{o} - F} = \frac{1}{(F^{o} - F')} + \frac{1}{K_{app}} \times \frac{1}{(F^{o} - F')[Ag]} \tag{13}$$

where K_{app} is the apparent association constant, F^{o} is the initial fluorescence intensity of dye molecules, F' is the fluorescence intensity of Ag adsorbed dye and F is the observed fluorescence intensity at its maximum. The calculated values of K_{app} obtained from the plot of $1/F^{o}$–F vs. 1/[Ag] (Fig. 10) are found to be 6.48×10^{8} for **3a** and $2.0 \times 10^{9}\ \mathrm{M}^{-1}$ for **3b**. The higher value of K_{app} indicates the strong association between the dyes and Ag NPs.

Conclusion

In summary, we have synthesized two chalcone derivatives, namely 3-(1-Benzyl-1*H*-3-indol-3-yl)-1-naphthalen-2-yl-propenone and 3-(1-Benzyl-1*H*-3-indol-3-yl)-1-thiophene-3-yl-propenone, with push–pull type system and structure of these compounds were identified by spectroscopy and single crystal X-ray crystallography. It is inferred from the absorption and emission spectra that emissive states of both compounds are of intramolecular charge transfer characteristics. For both the dyes the φf value shows sharp increase with increase in the polarity of the aprotic solvents and decrease in alcoholic solvents due to hydrogen bonding between solute and solvent. Physicochemical parameters such as molar absorptivity, oscillator strength, transition dipole moment and fluorescence quantum yield of both dyes have been calculated. The interactions of dyes with colloidal silver nanoparticles in ethanol have also been studied using fluorescence techniques. From the fluorescence quenching data, dynamic quenching and energy transfer from excited dyes to Ag NPs play a major role in the fluorescence quenching of dyes by Ag NPs.

Acknowledgments

The authors thank the Center of Excellence for Advanced Materials Research at King Abdul Aziz University for providing the research facilities.

Appendix A. Supplementary material

Supplementary data associated with this article can be found, in the online version, at http://dx.doi.org/10.1016/j.saa.2014.10.105.

References

[1] A.C. Arias, J.D. MacKenzie, I. McCulloch, J. Rivnay, A. Salleo, Chem. Rev. 110 (2010) 3–24.
[2] K.M. Rahulan, S. Balamurugan, K.S. Meena, G-Y. Yeap, C.C. Kanakam, Opt. LaserTechnol. 56 (2014) 142–145.
[3] Q. Li, M. Peng, H. Li, C. Zhong, L. Zhang, X. Cheng, X. Peng, Q. Wang, J. Qin, Z. Li, Org. Lett. 14 (2012) 2094–2097.
[4] Z.R. Grabowski, K. Rotkiewicz, W. Rettig, Chem. Rev. 103 (2003) 3899–4302.
[5] F.A.S. Chipem, A. Mishra, G. Krishnamoorthy, Phys. Chem. Chem. Phys. 14 (2012) 8775–8790.
[6] A. Hagfeldt, G. Boschloo, L. Sun, L. Kloo, H. Pettersson, Chem. Rev. 110 (2010) 6595–6663.
[7] H. Tian, X. Yang, R. Chen, R. Zhang, A. Hagfeldt, L. Sun, J. Phys. Chem. C 112 (2008) 11023–11033.
[8] Y. Suzuki, K. Komatsu, T. Kaino, Y. Honda, Opt. Mater. 2 (2003) 521–524.
[9] Y. Shi, W. Lin, D.J. Olson, J.H. Bechtel, H. Zhang, W.H. Steier, et al., Appl. Phys. Lett. 77 (2000) 1–3.
[10] M. Liu, P. Wilairat, M.L. Go, J. Med. Chem. 44 (2001) 4443.
[11] S.N. López, M.V. Castelli, S.A. Zacchino, J.N. Dominguez, G. Lobo, J. Charris-Charris, J.C. Cortes, J.C. Ribas, C. Devia, A.M. Rodriguez, R.D. Enriz, Bioorg. Med. Chem. 9 (2001) 1999.
[12] J.H. Wu, X.H. Wang, Y.H. Yi, Bioorg. Med. Chem. Lett. 13 (2003) 1813.
[13] L. Mathiesen, K.E. Malterud, R.B. Sund, Planta Med. 61 (1995) 515.
[14] T.A. Fayed, Chem. Phys. 324 (2006) 631–638.
[15] R. Chhabra, J. Sharma, H. Wang, S. Zou, S. Lin, H. Yan, S. Lindsay, Y. Liu, Nanotechnology 20 (2009) 485201.
[16] M.C. Daniel, D. Astruc, Chem. Rev 104 (2004) 293.
[17] W. Deng, E.M. Goldys, Langmuir 28 (2012) 10152.
[18] Y. Fu, J. Zhang, J.R. Lakowicz, J. Fluoresc. 17 (2007) 811.
[19] S. Kalele, A.C. Deshpande, S.B. Singh, S.K. Kulkarni, Bull. Mater. Sci. 31 (2008) 541.
[20] G. Raino, T. Stoferle, C. Park, H.C. Kim, T. Topuria, P.M. Rice, I.J. Chin, R.D. Miller, R.F. Mahrt, ACS Nano 5 (2011) 3536.
[21] M. Swierzewska, S. Lee, X. Chen, Phys. Chem. Chem. Phys. 13 (2011) 9929–9941.
[22] D.J. Maxwell, J.R. Taylor, S. Nie, J. Am. Chem. Soc. 124 (2002) 9606.
[23] H. Chung, P. Leung, D. Tsai, Optic. Exp. 22 (2013) 26483–26492.
[24] G.M. Sheldrick, Acta Cryst. Sec. A 64 (2007) 112–122.
[25] L.J. Barbour, J. Supra. Chem. 1 (2001) 189–191.
[26] J. Bernstein, R.E. Davis, L. Shimoni, N.L. Chang, Angew. Chem. Int. Ed. Engl. 34 (1995) 1555–1573.
[27] C. Reichardt, Chem. Rev. 94 (1994) 2319–2358.
[28] K. Rurack, M.I. Dekhtyar, J.L. Bricks, U. Resch-Genger, W. Retting, J. Phys. Chem. A 103 (1999) 9626–9635.
[29] J.B. Birks, Organic Molecular Photophysics, John Wiley and Sons, New York, 1973.
[30] S.A. El-Daly, A.M. Asiri, S.A. Khan, K.A. Alamry, J. Lumin. 134 (2013) 819–824.
[31] Z. Xu, G. Bai, C. Dong, Spectrochim. Acta Part A 62 (2005) 987–990.
[32] T.A. Fayed, M.A. El-morsi, M.N. El-Nahass, J. Photochem. Photobiol. A: Chem. 224 (2011) 38–45.
[33] E. Lippert, Z. Elektrochem 61 (1957) 962–975.

[34] N. Mataga, T. Kubota, Molecular Interactions and Electronic Spectra, Marcel Dekker, New York, 1970, pp. 371–410.

[35] P. Suppan, Chem. Phys. Lett. 94 (1983) 272.

[36] M. Ravi, T. Soujanya, A. Samanta, T.P. Radhakrishnan, J. Chem. Soc. Faraday Trans. 91 (1995) 2739–2742.

[37] B.J. Coe, J.A. Harris, I. Asselberghs, K. Clays, G. Olbrechts, A. Persoons, J.T. Hupp, R.C. Johnson, S.J. Coles, M.B. Hursthouse, K. Nakatani, Adv. Funct. Mater. 12 (2002) 110–116.

[38] P. Gordon, P. Gregory, Organic Chemistry in Colour, Chimia, Moskva, 1987.

[39] J.R. Lakowicz, Principles of Fluorescence Spectroscopy, third ed., Springer, New York, 2006.

[40] T. Förster, in: O. Sinanoglu (Ed.), Modern Quantum Chemistry, Academic Press, New York, 1996.

[41] H.A. Benesi, J.H. Hildebrand, J. Am. Chem. Soc. 71 (1949) 2703–2707.

Please cite this article in press as: M. Pannipara et al., Synthesis, spectral behaviour and photophysics of donor–acceptor kind of chalcones: Excited state intramolecular charge transfer and fluorescence quenching studies, Spectrochimica Acta Part A: Molecular and Biomolecular Spectroscopy (2014), http://dx.doi.org/10.1016/j.saa.2014.10.105